



Robotic assembly of modular concrete shells using falsework

Egor Ivaniuk^{a,*}, Dmytro Pukhkaiev^b, Mathias Reichle^c, Wanqi Zhao^b, Johannes Mey^b, Manuel Krombholz^b, Zlata Tošić^d, Uwe Aßmann^b, Sven Klinkel^c, Viktor Mechtcherine^a

^a TU Dresden, Institute of Construction Materials, Dresden, Germany

^b TU Dresden, Faculty of Computer Science, Software Technology Group, Dresden, Germany

^c RWTH Aachen University, Chair of Structural Analysis and Dynamics, Aachen, Germany

^d TU Dresden, Faculty of Mathematics, Institute of Geometry, Dresden, Germany

ARTICLE INFO

Keywords:

Concrete shell
Modular construction
Automated assembly
Digital construction
Model-driven software development
Isogeometric analysis
Scaled boundary method

ABSTRACT

The rapid development of robotics has the potential to transform the construction industry of the future. One possible application of robots is the assembly of modular concrete shells. This type of structure saves materials, while the modular approach makes them more cost-effective by eliminating the need for formwork. So far, however, robots have struggled to accurately position modules when assembling large modular shells on the construction site. The authors propose an alternative approach to the robotic assembly of modular shells based on the use of modular falsework. The presence of a falsework enables the creation of large-scale shells of complex shapes out of an unlimited number of modules while ensuring the accuracy of their positioning. This paper describes a possible methodology for implementing this approach and validates it by assembling a demonstrator, as well as presents the results of static and dynamic analysis of the modules moved by the robot.

1. Introduction

Concrete shells have been known for centuries as efficient structures to achieve savings in building materials. They allow large areas to be covered without the use of internal supports, providing the open interior required in a variety of structures including sports arenas, exhibition halls, hangars, and warehouses. Furthermore, they can be designed relatively thin, provided that the forces in the structure are transmitted mainly by the membrane action. Such structures would be beneficial nowadays when the rational use of resources in construction is more important than ever: The global community is focused on reducing the negative environmental impact of mankind, while cement production is responsible for 10 percent of total carbon dioxide emissions (Scrivener et al., 2018). At present time, however, concrete shells are rarely erected, and the main reason for this is the conventional approach to their construction. It requires the creation of complex curved formwork, which is an expensive and labor-intensive process. Such formwork is generally used only once and has to be disposed of after construction.

Over the years, several alternative methods have been proposed for the construction of concrete shells on-site (Schipper, 2015; Vatandoost et al., 2024), however, nearly all of them have their disadvantages. Some of these methods are labor-intensive (soil and ice formwork,

ferrocement (Vatandoost et al., 2024)), and in some others, it is difficult to predict the final geometry of the structure due to the sagging of the formwork under the weight of the concrete (grid shell, cable-net, fabric, and pneumatic formwork (Hawkins et al., 2016)). There is also a group of methods that impose constraints on the geometry of the structure (pneumatic formwork and Pneumatic Forming of Hardened Concrete (Kromoser and Huber, 2016)).

Modular shell construction is an alternative approach that not only solves the problems associated with the conventional technique by eliminating the need for formwork but also overcomes the disadvantages of other alternative methods by providing a wide range of available geometries and high geometric accuracy. In this approach, individual modules are fabricated in a factory and subsequently assembled into a shell on-site (Oval et al., 2023). The similarity of the prefabricated shell modules enables a high level of automation and quality control in the production process, while simultaneously reducing waste. Compared to the conventional formwork-based approach, modular construction requires much more complex transportation coordination and planning of all its stages, but ultimately reduces the price and construction time (Shamshiri et al., 2019; Hammad and Akbarnezhad, 2017). According to Straten (Straten G van der, 2018), prefabrication can accelerate the construction time of concrete shells from 2

* Corresponding author.

E-mail address: egor.ivaniuk@tu-dresden.de (E. Ivaniuk).

and up to 6 times depending on the chosen module connection technique. In addition, the modular approach facilitates circular design and reduces noise (Hořínková, 2021).

The problem that prevents this method from becoming widespread is the difficulty of assembling the modules into a final structure. The geometric nonlinearity of the shell complicates the positioning of the modules. Furthermore, in the intermediate stages of construction, additional temporary supports are usually required to ensure the stability of the partially assembled structure. The complexity of assembling modular shells can be addressed through the use of robots. Automation has already improved the productivity of many manufacturing industries, and research into its application in the construction industry has recently been actively pursued (Bock, 2015). Automating the assembly of modular shells can increase the efficiency of their construction, making them more attractive to investors, while ensuring a high level of precision and on-site safety.

There are currently no examples of robots being used to assemble modular concrete shells known to the authors, however, several studies have demonstrated the feasibility of using robots to assemble modular shells made of other materials. Shilova et al. (2018) used a robotic arm to create shells from styrofoam modules. The use of temporary supports was avoided due to the lightness of the material used and the special geometry of the module edges, which ensured their mutual interlocking.

In several studies, additional robots have been used to support a partially erected structure. In the research by Bruun et al. (2021) two robots worked together to assemble a central arch of a 2.2 m high and 4.4 m long glass masonry vault, taking turns either supporting the partially assembled structure or installing a new module. Similar cooperative work between the two robots was also demonstrated by Wang et al. (2023) during the assembly of small-scale modular shells made of plastic. The use of robots as temporary supports, however, imposes restrictions on the geometries of the shells to be erected. Only special assembly-oriented designs are suitable for this approach, in which the number of temporary supports required should not exceed the number of additional robots used.

Another approach, involving the use of two robots to assemble a modular shell was demonstrated by the University of Stuttgart (Lauer et al., 2023). In that project, two manipulators were used to assemble a shell with a free span of around 16 m directly on the construction site. The structure was made of wooden modules, which made it possible to use screws to connect them with each other during assembly, thus avoiding the use of temporary supports. However, during assembly, it was discovered that uncontrolled site conditions led to errors in the positioning of the modules by the robot.

Thus, it can be concluded that in previous studies, although it was possible to automate the assembly of modular shells without the use of formwork, this was only achieved by severely restricting the geometry of

the shells to be built or by using lightweight and easily connectible modules. Robotic assembly of large-scale modular concrete shells (see Fig. 1) requires a special approach. It is difficult to accomplish it without the use of additional supports, as concrete modules are heavy compared to other materials, and high moments can occur at the joints when the modules are cantilevered. The use of robots as supports is complicated by the fact that the heavy weight of the modules increases the positioning error. In addition, as the required number of supports to be used simultaneously typically increases with the size and complexity of the structure geometry, the use of robots for this might become impractical. Alternatively, supports may be provided by cables or chains attached to the modules at one end and to cranes or towers at the other (Deuss et al., 2014), however, with this approach, it is also difficult to accurately position the modules under unstable conditions of the construction site.

The solution to this problem can be the construction of falsework, on which the modules will rest during the assembly. This approach was successfully implemented in the construction of a tile vault prototype at ETH Zurich (Davis et al., 2012), where CNC-cut cardboard boxes were used as a falsework. The shape of the prototype vault was defined using the RhinoVAULT plugin for Rhino Grasshopper (Rippmann et al., 2012). To avoid asymmetrical loads on the vault during falsework disassembly, it was built on cardboard spacers sealed with plastic tubes. After the vault was completed, these tubes were filled with water, which dissolved the non-water-resistant cardboard glue. As a result, the spacers began to gradually compress under the weight of the pallets, allowing the entire falsework to be lowered evenly. In that study, however, the assembly and disassembly of the falsework as well as the assembly of the tile vault was done manually.

The authors of this paper propose a new method for the automated construction of modular concrete shells based on the robotic assembly of reusable falsework. In this approach, a falsework is first assembled by one or more robots. It consists of individual modules allowing different geometries to be created. The falsework is then used to provide support for the modules of the concrete shell during their assembly. In contrast to the formwork with a surface that follows the geometry of the shell used in the conventional construction approach based on the pouring of fresh concrete, the falsework only provides support at individual points, which, however, is sufficient when working with hardened concrete. After completion of the construction, the falsework is dismantled and can be reused. Although shell assembly using the proposed approach is more time-consuming than other automated approaches that do not require falsework, it has the potential to enable full automation of construction, ensuring high accuracy of module positioning without imposing restrictions on the geometry of the shells. Table 1 presents a comparison of different shell construction methods, such as the conventional formwork-based method and two automated methods based on the modular approach, including the formwork-free method, which uses an additional robot as temporary support, and the falsework-based method proposed in this publication.

The objectives of this paper are to demonstrate the feasibility of the proposed method of assembly of modular shells, as well as to evaluate the stresses and deformations that may occur in the modules during the assembly process. The next section of the article outlines the state of the art in modular shell design, concrete module fabrication, and robot-assisted assembly. Section 3 describes the methods used to program the robot for automated falsework and shell assembly and to detect critical states in the modules during the assembly process. Section 4 presents the results and discussion of the conducted experiments on the automated assembly of the modular shell according to the proposed method as well as the performed numerical analysis of the modules. Finally, Section 5 summarizes the findings of the publication and outlines possible directions for further research.

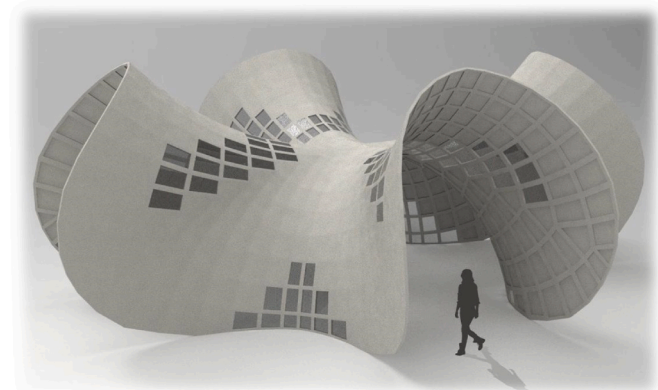


Fig. 1. Example of the design of a large-scale modular concrete shell (Tošić et al., 2022).

Table 1
Comparison of shell construction methods.

Parameters	Construction method		
	Conventional formwork-based	Automated formwork-free	Automated falsework-based
Automation level	●	●●●	●●●●
Construction speed	●	●●●	●●
Cost savings	●	●●	●●
Geometric freedom	●●●	●	●●●
Precision	●●●	●	●●
Waste reduction	●	●●●	●●●

● - low,
●● - medium,
●●● - high

2. State-of-the-art design, fabrication, and assembly of modular shells

2.1. Parametric modularization of the shell

The special design and segmentation strategies for the assembly of modular shell structures are determined by the conditions at the local level of the module geometry originating from the used manufacturing technology. This approach is known as the production-aware design of shell structures and involves various methods and strategies depending on the used production method and project demands (Costa et al., 2021). These local conditions can be determined through the specific limitations of the size, shape, weight, and number of the modules in the construction which can be crucial for the production as well as for the robotic assembly process. Depending on the project conditions, two different approaches can be used: post-rationalization and pre-rationalization (Douthé et al., 2017). Post-rationalization is the implementation of modularization methods on the already given design (Tošić et al., 2022; Dimčić, 2011). Pre-rationalization starts from carefully selected geometry that has embedded important geometric (Pellis et al., 2021; Abdelmagid et al., 2023) or structural properties (Block and Ochsendorf, 2007; Bhooshan et al., 2022).

Several approaches to the design and segmentation of modular shells have been demonstrated to this point. They are mainly focused on arch-like designs within the complex shapes of modular structures, allowing for falsework-free assembly. Regarding structural properties, emphasis is placed on compression-only structures due to their ability to accommodate dry joints and transmit compression forces exclusively, mitigating joint-related issues. Quad, hexagonal, and polygonal segmentation topologies are favored, as they provide multiple attached edges during module assembly, enhancing stability.

Kao et al. (2017) proposed a workflow for assembly-aware design of masonry shell structures, introducing an interactive CAD tool to simulate the step-by-step assembly of masonry blocks and explore the design space. The research extends the workflow with four key steps: generating a form-found surface, tessellating it into block geometry, creating an assembly sequence based on backward assembly planning, and iterating until a feasible solution is found. The authors compared three main

topologies (i.e. triangular, quad, and polygonal) and concluded that the last one has the best stability and force transmission during the assembly sequence. Another approach was demonstrated at the University of Stuttgart, where a co-design workflow was developed and applied for the design of a modular shell named BUGA Wood Pavilion (Wagner et al., 2020). An agent-based modeling method (Groenewolt et al., 2018) was used for segmentation in accordance with production and assembly conditions. Paris et al. (2021) demonstrated the use of the Discrete Element Method for calculating the stability of a glass masonry vault at all the stages of robotic assembly. Shah et al. (2022) developed an assembly-oriented design methodology for segmented timber shells with robots. The design concept contains an exploration of design planarization with hexagonal modules, while the assembly is based on the segmentation of the given design (Pluta et al., 2021). Particular attention was paid to the directions of segmentation into modules. These are directly influenced by the assembly sequences creating secondary arches within the designed shape as a temporary support structure, which are created based on the principal stress directions and support points. Wang et al. (2023) proposed a design-to-fabrication workflow that enabled the automated construction of discrete assemblies without the need for additional falsework. It was possible to implement this approach for the construction of compression-only dome-like modular shells, which were designed by utilizing a form-finding process using the Kangaroo2 plugin for Rhino Grasshopper. The segmentation strategy was formulated based on the inclination of the interfaces of dry joints between modules. For a stability evaluation, the Coupled Rigid-Block Analysis method was implemented (Kao et al., 2022).

This research focuses on the use of falsework for the assembly of modular shells. In contrast to methods focused on falsework-free assembly, the proposed approach does not impose strict limitations on the available geometries of the shells to be erected, but the positions of the temporary supports to be installed must be planned during the design process. Falsework structure can be optimized, as demonstrated by Luitse and Eigenraam (2017), who developed an algorithm that can significantly reduce the amount of temporary supports needed. In addition, the stresses occurring in the modules during the robotic assembly process must be considered, which will be demonstrated in Section 4.3. Moreover, the assembly order can be optimized to reduce robot movements, thereby decreasing the construction time.

2.2. Design of the joints

The methods of connecting shell structure modules can be categorized into three groups. The first group is based on the mechanical interlocking between the modules, which involves machining protrusions on one module and corresponding indentations on the adjacent module (Oval et al., 2023; Rippmann et al., 2018). These types of connections are well suited for automation but require very high geometric accuracy of the manufactured modules to ensure a quality joint and avoid high localized loads. It also requires a constant force to press the modules against each other, therefore this type of connection is often used in conjunction with post-tensioning.

The second group of methods provides a non-detachable connection and includes methods such as welding, grouting, and adhesive bonding. Welding involves the incorporation of steel elements into the modules during their manufacture. The other two methods have no prerequisites but may require time to cure (Kumar et al., 2017). The widespread use of technologies such as robotic welding, 3D concrete printing, and robotic gluing suggests that these types of joints can also be automated in the near future.

The third group of methods uses mechanical fasteners to create detachable joints. Fasteners can be embedded in the concrete during casting (Peters et al., 2017) or, as an alternative, can be attached to the modules with anchors. The modules can be bolted together using special connectors (BT-Spannschloss®). Another approach is to tie the modules together using steel cables placed in the modules during the

manufacturing process and fixed in specially prepared holes in the neighboring module (Ivaniuk et al., 2022a). This group of connections is the most difficult to automate and is currently unlikely to be applied without human assistance.

2.3. Fabrication of the modules

Two main approaches are applied to the creation of concrete shell modules. The first is the casting of concrete into standard formwork, which can be produced, for example, using CNC-milling (Dombrowsky and Sondergaard, 2009) or hot-wire cutting (Stavric and Kaftan, 2012). This approach allows modules to be produced with great precision, but the formwork production process is time-consuming and often generates considerable waste. It is to be mentioned that several approaches have been presented that allow the creation of formwork without waste, by using wax (Mainka et al., 2017), frozen sand (Gericke et al., 2016), or ice (Sitnikov, 2019) for this purpose.

The second and more innovative approach is the casting of concrete in an adaptive mold (Schipper et al., 2014). This is a device that consists of a grid of actuators, capable of moving vertically, and an elastic surface fixed on top of them, on which the concrete modules are manufactured. The adaptive mold can be used to create modules of different geometries without waste. However, often in the presented studies the module boundaries were placed manually, which significantly reduced the level of automation of the production process. This problem can be solved by using 3D printing technology to create edges of the modules.

A method for the fully automated production of reinforced modules of concrete shells using 3D printing has been proposed by the authors of this paper within the Adaptive Concrete Diamond Construction (ACDC) project (Ivaniuk et al., 2022b, 2024). The method proposed in the project is based on flow production, in which modules are moved between stations in which sub-processes of their production are carried out. As the initial step, the first layer of the module contour is printed and filled with flowable concrete, then the reinforcing mesh is placed on it, after which the second layer of the contour is printed and filled with flowable concrete. It is also possible to create lightweight frame modules without concrete filling. Fig. 2 shows a demonstrator consisting of both types of modules fabricated using the proposed technology.

The reinforcing mesh provides structural reinforcement, while the edges of the modules are printed using Strain Hardening Cementitious Composite (SHCC). This material, reinforced with short polyethylene fibers (Ivaniuk et al., 2022c), allows the modules to withstand not only quasi-static loads occurring in the shell but also dynamic concentrated loads that may occur during transportation and assembly.

The initial phase of the ACDC project focused on planar modules, but



Fig. 2. Concrete shell consisting of filled and frame modules (Ivaniuk et al., 2024).

the feasibility of applying the proposed approach to create curved modules using adaptive mold is being investigated. The combined use of this module production technology and the robotic module assembly technology proposed in this paper can enable full automation of the concrete shell construction process.

2.4. Automated robot-assisted assembly

Automated assembly of modular shell structures is a special case of a more general problem known as *automated assembly*. Automated assembly systems play a crucial role in a transition to smart manufacturing by enabling efficient and precise integration of components and materials into complete products, as well as integration of subsystems into a modular assembly line, thereby streamlining production processes and improving product quality. Assembly systems should demonstrate enhanced responsiveness due to the growing demand for customized products, which requires the ability to efficiently accommodate and integrate a wide range of product varieties (ElMaraghy and ElMaraghy, 2016; Manzini et al., 2018).

To efficiently construct a complex assembly line, it is often necessary to break the whole line down into smaller work cells and coordinate their activities through inter-cell communication and collaboration, as suggested in (Aghazadeh et al., 2011). For constructing such a modular and reconfigurable assembly line, the ISO 15531 PPR (Process-Product-Resource) model serves as a fundamental guide (Cutting-Decelle et al., 2007). Numerous issues must be considered, for instance, the product's structure and attributes, which can be specified through various methods such as CAD models (Lupinetti et al., 2019) or knowledge graphs (Chen et al., 2020), but also be obtained by feature extraction (Hadj et al., 2018) in machine learning. Based on this, the assembly system can represent relations between components and materials using Liaison Graphs (De Fazio and Whitney, 1987), And/Or Graphs (Homem de Mello and Sanderson, 2002), feature-based representations on connective-relation graphs (Gu and Yan, 1995), or an Assembly Interference Matrix (AIM) (Dini and Santochi, 1992). Based on these relations between components and materials, several algorithms can be used to generate assembly sequences, such as genetic algorithm-based methods (Lazzerini and Marcelloni, 2000), graph decomposition methods (Homem de Mello and Sanderson, 1988), and tree search (Sung and Corney).

To improve productivity and increase the level of automation in manufacturing, it is essential to integrate robots into the assembly lines and optimize the assembly workflows. *Robotic assembly* has been an active area of research, with studies focusing on various independent tasks such as LEGO assembly (Nägele et al., 2024), furniture assembly (Knepper et al., 2013), and plug-in tasks (Park et al., 2017). To enable robots to perform these assembly tasks, several methods have been proposed for teaching and training them. One approach is to learn from human demonstrations (Liu et al., 2023), where robots observe and mimic the actions performed by human operators. Another promising method is to use virtual reality (VR) demonstrations (Zhang et al., 2021), which provide an intuitive and immersive environment for teaching robots assembly skills.

Given the intricacy of developing a system for assembly tasks, it is crucial to have a well-structured approach for integrating PPR models with robots. To this end, model-driven software development (MDS), a software design and development methodology, can be employed. It involves creating abstract models of software systems, checking them on consistency and other quality properties, and then systematically transforming them into concrete implementations (Schlegel et al., 2009). Several directions of MDS have emerged in robot modeling research, including skill-based models for skill specification (Rovida et al., 2017), domain-specific languages (DSL) for appropriate formulation of robotic tasks (Nordmann et al., 2014), and the model-driven architecture (MDA) for distinguishing platform-dependent from platform-independent models (Beaulieu et al., 2018). Furthermore,

MDSO research has explored various approaches to quality-check the products and resources: ontologies for constraint-based modeling (Ahmad, 2017), knowledge-based models for intentional specifications (Ahmad et al., 2018), and feature-based models for hierarchical variant specifications (Holland and Bronsvort, 2000). To utilize the quality checks of MDSO also for robot-assisted assembly, MDSO techniques for formal languages such as Petri Nets (Ebert et al., 2023, 2024), timed automata (Dehnavi et al., 2019), or context-sensitive grammars (Dantam et al., 2011) should be employed.

Also, sophisticated distributed software platforms are needed. In the field of robotics, the Robot Operating System (ROS) (Macenski et al., 2022) offers (at least, since version ROS 2) an industry-grade middleware with advanced communication features such as Quality-of-Service (QoS) and real-time specifications, as well as a rich software ecosystem. In the context of construction, ROS can be employed for the planning of trajectories in automated assembly. The MoveIt framework (Coleman et al., 2014) of ROS supports exchangeable motion planning algorithms, offers a simulation environment, and frameworks for computing grasp poses (ten Pas et al., 2017). On top of these trajectory planners, frameworks to plan entire tasks are offered, e.g., the MoveIt Task Constructor (Görner et al., 2019), which uses behavior-trees for actions with attribution and data-flow-centered sampling methods.

3. Methods

3.1. Approach for automatic robot-assisted shell assembly

3.1.1. RobotRAGs: approach for general-purpose robot-assisted assembly

Our approach for automatic robot-assisted shell assembly is based on RobotRAGs (Zhao et al., 2023), a model-driven approach for developing robotic assembly systems using a special form of context-sensitive grammars, Relational Reference Attribute Grammars (RAGs). RobotRAG provides a modular, extensible approach to specify how to integrate robots into assembly lines that can accommodate diverse domains. RobotRAGs consist of three domain models, each being a partonomy, i. e., the whole-part hierarchy of objects including inner links (Mey et al., 2020). The *RobotCapabilityModel* defines the capabilities, skills, and constraints of the robots used in the assembly process. The *WorkCell* model represents the physical environment and elements involved in the assembly process. It contains multiple *WorkArea* entities, each focusing on a different aspect of a particular product. The *WorkArea* includes a *ProductModel* that defines the structure and parts of the product being assembled (*GoalProduct*) and the current assembly status (*CurrentState*).

The goal product is partitioned into discrete *ProductLayers* from bottom to top, with each *ProductLayer* containing one or more *ComponentGroups*. A *ComponentGroup* consists of individual *Components* and *Connections* between them. Finally, the *ActionModel* represents the assembly planning and execution. It is derived from the *GoalProduct* in the *WorkCell* and adapted to the available robots defined in the *RobotCapabilityModel*. The model assigns robots with the appropriate skills to execute actions.

Using Relational RAG supports modularity, enables the separation of concerns, and facilitates the accommodation of changes in requirements, materials, and robot capabilities (self-adaptation). The Monitor-Analyze-Plan-Execute (MAPE) loop, a central part of the RobotRAG, enables the system to monitor the assembly process, analyze the goal product, plan actions using the models, and execute them using the available robots. The use of relational RAGs enables the extension of the models to incorporate additional features and constraints as needed for specific applications. Fig. 3 shows the assembly process of RobotRAGs.

3.1.2. ShellAssemblyRobotRAGs: approach for automatic robot-assisted shell assembly

In this paper, we offer an extension to RobotRAGs called ShellAssemblyRobotRAGs, which adapts them to the context of automatic robot-assisted shell assembly. The main workflow for shell assembly consists of three steps (see Fig. 4a).

First, the CAD models of the falsework and the shell structure are integrated into the simulation software. Second, an instance of RobotRAGs performs the simulated assembly of the shell structure. Third, the real-world assembly of the shell structure is carried out using the same, already simulated instance; the only adjustment required is to change the communication interface from the simulation to the real robots. In the ROS application, this can be achieved by modifying the launch file.

To minimize the difference between the simulation environment and the real-world assembly, we perform it with a physical engine Gazebo (Gazebo. https). However, the complete identity of simulation and physical environments cannot be guaranteed due to unpredictable hardware failures and malfunctions. Therefore, an error compensation mechanism is necessary to recover from such events. We consider the development of such a mechanism as a promising direction for future work.

The core process of shell assembly (see Fig. 4b) is identical for simulated and real-world cases (see Fig. 4a), but extends the basic RobotRAG approach (see Fig. 3). Instead of considering only product assembly, the extended method ShellAssemblyRobotRAGs comprises

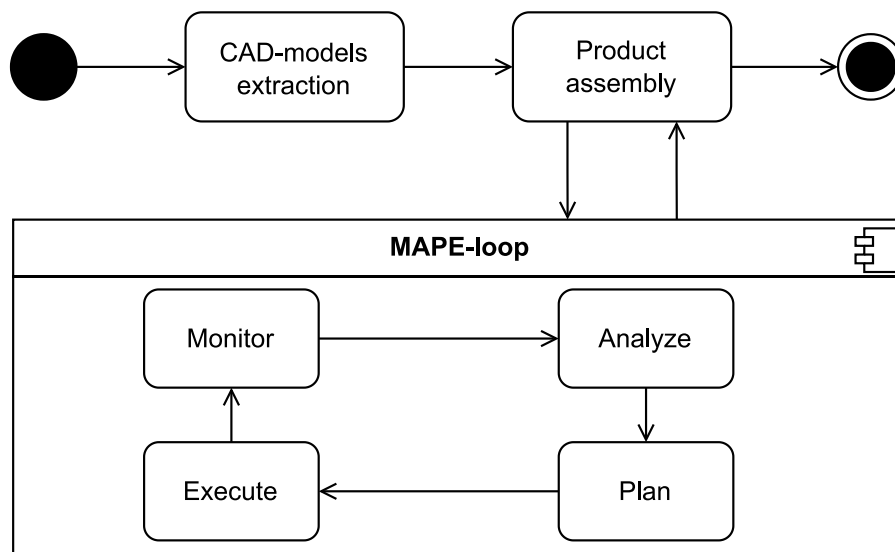


Fig. 3. The process of robot-assisted assembly using RobotRAGs.

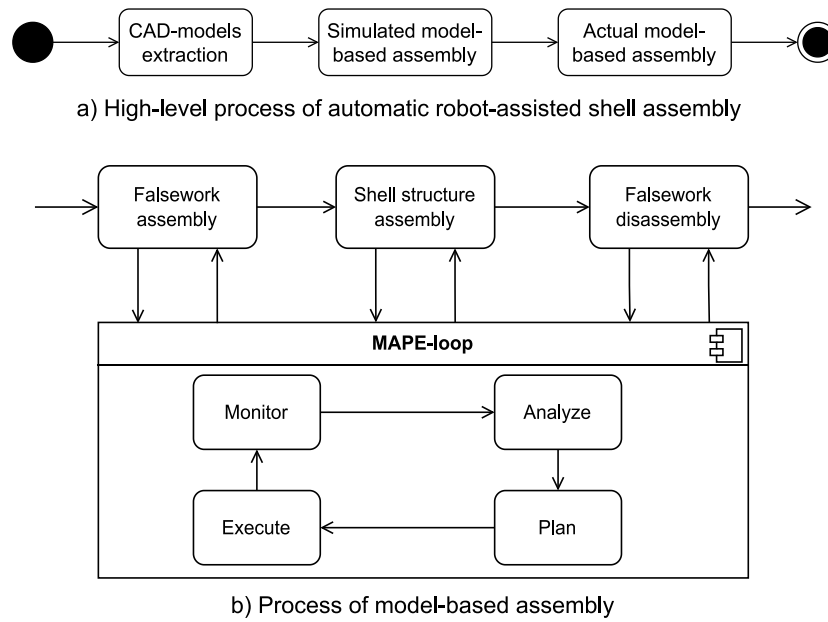


Fig. 4. A model-based engineering approach for automatic robot-assisted shell assembly. The processes of simulated and actual assembly are identical.

three activities:

- 1) *Falsework assembly*, exposing spatial support points for the shell structure.
- 2) *Shell structure assembly*, exploiting the support points to avoid bending, tipping over, and collapsing of the shell structure during assembly.
- 3) *Falsework disassembly*, leading to the final state of the shell structure.

ShellAssemblyRobotRAGs have several important advantages for shell assembly. Firstly, the MAPE-loop is shared between the aforementioned activities, leading to their interaction. For example, if the approach acknowledges that the envisioned shell structure cannot be assembled with the current shape of the falsework, the MAPE-loop has to enact a reassembly of the falsework. Secondly, the assembly of the falsework can be performed out of the box by the initial RobotRAGs approach, however, several adjustments are necessary. On the one hand, the gripping side of each shell (treated as a *Component* by RobotRAGs) and the pose of the end-effector must be dynamically detected. Here, the vulnerability of the modules must be respected, which can be pre-computed by a structural analysis that considers all states that the module undergoes during construction. Consequently, recommendations and warnings can be given to maintain the health of the modules (see Section 3.2). On the other hand, the connection of the modules must be considered (see Section 2.2). Thirdly, RobotRAGs are, in general, able to plan the disassembly of the falsework, since the structure of the assembled product is recorded in the model. After synchronizing with the real-world post-assembly status, the system can easily plan the disassembly sequences of the falsework taking this status information into account. It may also adjust the gripper orientation to avoid collisions between the assembled product and the robot arm. The status of this planning is discussed in Section 4.

3.2. Detection of critical states in the modules during assembly

During the assembly of modular shells not only the correct assemblage is of relevance, but also the vulnerability of the modules needs to be considered. In fact, damaged or cracked concrete modules can highly affect the stability and load capacity of the structure and in the ultimate state lead to a collapse of the system. Therefore, the detection of critical states during the assembly is inevitable to ensure the structure's

stability.

Both fill and frame modules can be used to assemble the modular shell, see Section 2.3. Thanks to the large smooth surface, the filled modules can be moved with a robot equipped with a vacuum gripper (Lauer et al., 2023), which can also work on curved surfaces (Gabriel et al., 2020). The module can be held by its center, thus avoiding high stresses. Frame modules can be moved using the commonly used two-jaw parallel gripper by grabbing the module by its side edge, however, the possible stresses and deformations that will occur in the module must be taken into account. In addition, since during the assembly process each module undergoes several orientation and loading states due to robot motion, the detection of the critical states must be evaluated during motion planning.

As the assembly process demands a high precision for the correct placement and movement of the modules, the numerical model to detect the critical states and movement of the modules, the numerical model to detect the critical states needs to match the requirements in precision. For this reason, the method of scaled boundary isogeometric analysis (SB-IGA) was chosen (Chasapi and Klinkel, 2018; Arioli et al., 2019). The method combines the advantages of the isogeometric analysis (IGA), which provides the opportunity for precise geometry description and high-order continuity in the interior domain, with the scaled boundary (SB) method, which is a boundary-oriented method to describe a domain by its boundary. It relies on a boundary curve, defined by B-splines or NURBS (Non-Uniform Rational B-Splines), and a central point in the domain of interest, called the scaling center. The parameterization of the domain is defined as:

$$x = x_0 + \xi (x_s(\eta) - x_0) \text{ for } \xi \in [0, 1] \quad (1)$$

where x_0 are the coordinates of the scaling center and x_s is the boundary curve. The parameter η denotes the parameter space of the NURBS curve, while ξ is the scaling parameter, scaling from the scaling center to the boundary curve in the limits of 0 (at the scaling center) and 1 (at the boundary). It is important to note, that in plate and shell analysis, the scaling strategy considered herein is referred to as the “radial”/in-plane scaling strategy, which is fundamentally different from the “normal” scaling strategy (Man et al., 2013; Reichle et al., 2024). This yields that the design model for the construction can be utilized as the basis of the parametrization. Since the design model of the modules is defined by NURBS curves in a kind of a “Wireframe Model” the workflow as a pipeline from model to structural analysis is possible without loss of

geometric information. Fig. 5 shows the design of a modular concrete shell taken for parametrization. Indeed, an infill of the shell modules increases the rigidity and the load-bearing capacity, but it also increases the weight of the structure significantly. Therefore, the modular shells are restricted to concrete shells without infill. As the approach does not have any restrictions with respect to the number of boundary curves, a parametrization of modules with infill is possible in a straightforward way. The authors want to remark that a requirement of the scaled boundary method is that the parametrized domain needs to be star-shaped. For any domain, a scaled boundary parametrization is possible by subdivision into star-shaped blocks, see (Bauer et al., 2021). Herein, the modules are defined by the boundary lines on the middle surface and are decomposed into several blocks to preserve starshapedness.

In terms of the analysis of thin-walled structures, the application of SB-IGA was recently presented for Kirchhoff theory in plates (Arf et al., 2023) and shells (Reichle et al., 2023). Therein C^1 continuity across the subdomains is obtained by considering the analysis-suitable G^1 parametrization for smooth domains which yields that Kirchhoff theory can be used as the weak form of the mechanical problem. The load is applied in a quasi-static approach and the stresses and deformations are obtained from solving the problem at critical states of the assembly. Consequently, evaluating the (bending) stresses, the critical states can be found if the stresses exceed the tension strength of the uncracked concrete. In the load cases the module faces during the assembly, membrane stresses are negligibly low compared to bending stresses. If the stresses exceed the load-bearing capacity of the module, a critical state of the assembly is found and recommendations can be given to the robot.

4. Results and discussion

4.1. Demonstrator “Archi-like shell”

A demonstrator has been created to show the feasibility of the robotic assembly of modular shells by the proposed falsework-based method. The design of the demonstrator was developed as a scaled-down version of a modular arch presented in (Ivaniuk et al., 2024) and shown in Fig. 2. The demonstrator has a span of 600 mm and a height of 300 mm, consisting of two strips of 7 modules each, see Fig. 6. The dimensions of the demonstrator were chosen to ensure accessibility to it from all sides by the robot used for its assembly. In contrast to its predecessor, the small-scale demonstrator consists only of frame modules, which allows it to be completely assembled using only one type of robot end effector. The method of connection between the modules has also changed. Modules of large-scale demonstrator were connected with each other by

steel bolts and cables, which is difficult to accomplish without human assistance. Therefore, to realize the possibility of fully automated assembly, the connection between the modules in the small-scale demonstrator was carried out using magnets. They significantly facilitate the automation of modular shell assembly, simplifying the process of module connection while ensuring the accuracy of their mutual positioning. However, it is important to acknowledge that they are unable to match the strength and durability of mechanical fasteners, and thus can hardly be employed as the single connection method for the construction of full-scale modular shells.

In the designed small-scale demonstrator, the width of the module edges was about 13 mm, which did not allow printing them using the available 3D concrete printer, capable of printing layers with a width starting from 40 mm. Therefore, the demonstrator modules were created using a 3D-printed plastic stay-in-place formwork filled with self-compacting concrete. The first stage involved 3D printing of plastic formwork with holes in the side edges into which magnets were placed, see Fig. 6a. The polarity of the magnets was chosen to ensure the mutual attraction of adjacent arch modules. Afterward, a self-compacting concrete with a maximum aggregate size of 2 mm was poured into the printing formwork through a funnel, see Fig. 6b.

4.2. A feasibility study for robot-assisted assembly

In our feasibility study, we experimented with the automation of an important subset of the activities introduced in Section 3.1, namely model-based falsework assembly (Activity 1) and guidance-based shell structure assembly (Activity 2). Disassembly of the shell structure is currently under further experimentation and it is expected that Activity 3) can be integrated in the near future.

4.2.1. Falsework assembly (Activity 1)

The *Falsework Assembly* for the arch-like shell was organized with a *ShellAssemblyRobotRAG* assembling Asago magnetic stones, running on a Franka Emika robot. These game stones use the same 3D cubic pattern with sides of equal length. They comprise a magnetic joint mechanism that is easy to join-in and easy to click-out, see Fig. 7 (right). They also are of low weight so the gripping with the Franka robot is simple. The stones can be assembled layer by layer, as required by a *ShellAssemblyRobotRAG*. Every Asago stone is a *Component* in the *ShellAssemblyRobotRAG*, which, when grouped, becomes part of a *ComponentGroup*. The falsework grows layer by layer, *ComponentGroup* by *ComponentGroup*, until the desired height is reached.

Spatial support points of the falsework are pre-designed in the *GoalProduct* of the *ShellAssemblyRobotRAG*, so that in Activity 2, the

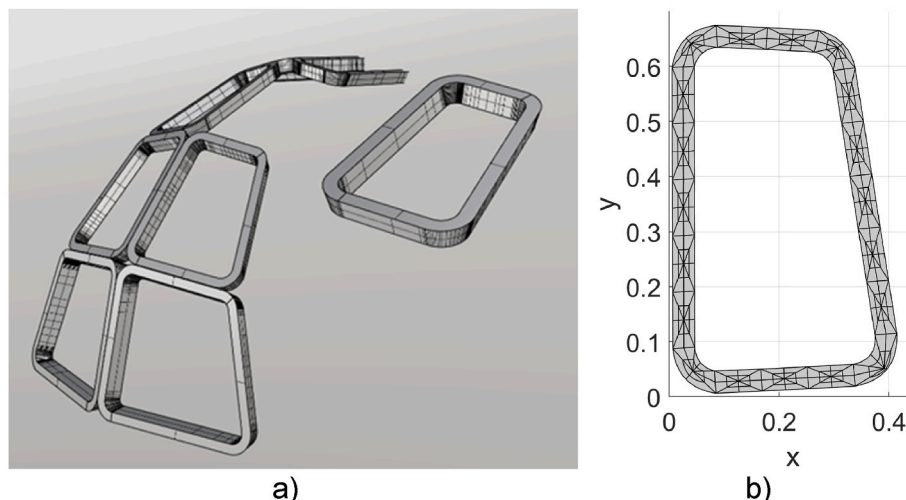


Fig. 5. a) Geometry of a single module, and b) SB-parametrization of the module.

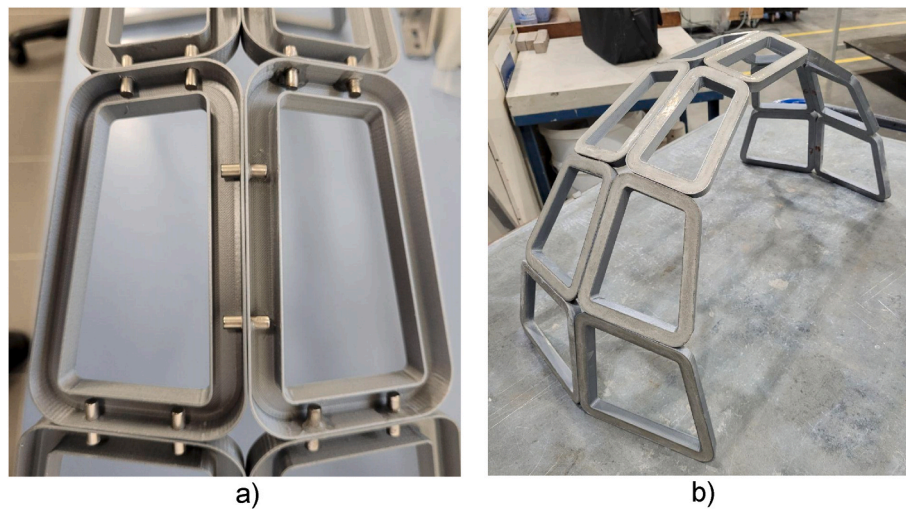


Fig. 6. a) 3D-printed plastic stay-in-place formwork for manufacturing modules with installed magnets and b) modules after the concrete has been poured and cured, assembled into an arch-like shell.

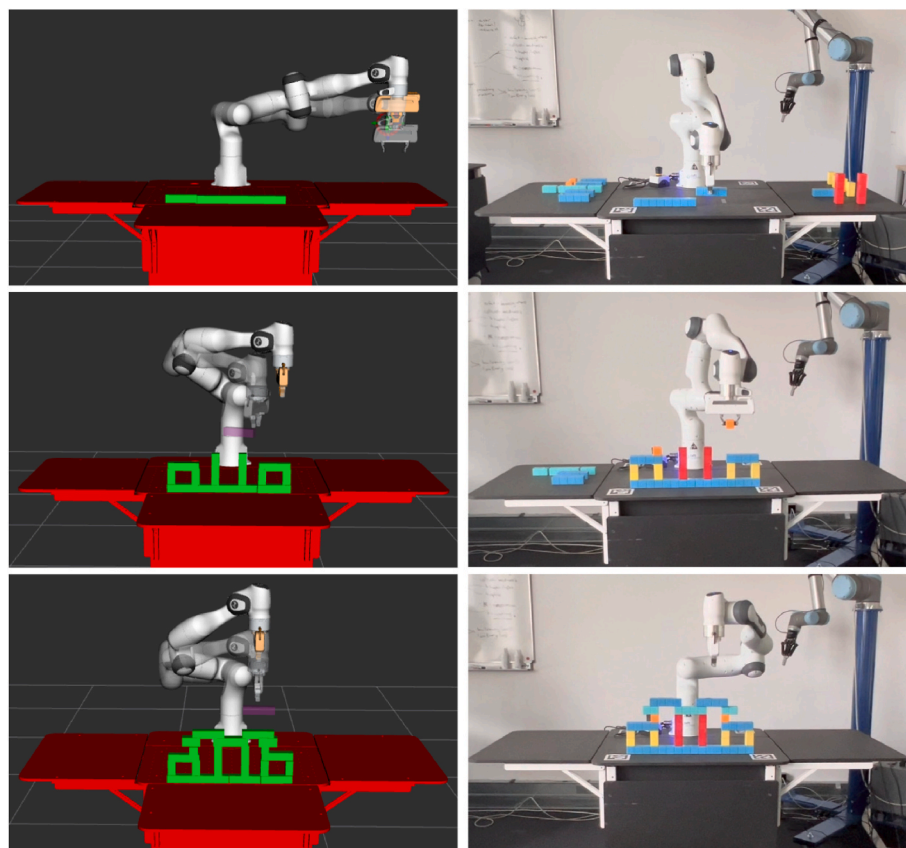


Fig. 7. Steps of simulated (left) and actual (right) assembly of the falsework.

shell-module assembly, the support points can be laid on by modules. To this end, every spatial support point is covered by a peak of the falsework, in the way that a corresponding *ComponentGroup* is arranged to spatially cover the support point. For instance, the support point SP1 shown in Fig. 8 is designed to be assembled as *AtomicComponent* AC1 in *ComponentGroup* CG1 on *ProductLayer* PL1. On this support point SP1, a shell module will be laid during the Structure Assembly.

For the presented demonstrator, the falsework assembly task involves 19 components. The process is broken down into individual steps, each consisting of a pick-and-place action. Step durations range from 15

to 43 s, averaging 26 s per step, with a total assembly time of 497 s.

Clearly, the Asago game stones used to create the falsework are not suitable for assembling large modular shells. This would require the development of larger modules made of more durable materials, as well as another, more suitable method of connection between the modules. One possible approach could be to use steel modular frames similar to those proposed by Sun et al. (2022) or those used for volumetric modular construction of buildings (Liew et al., 2019).

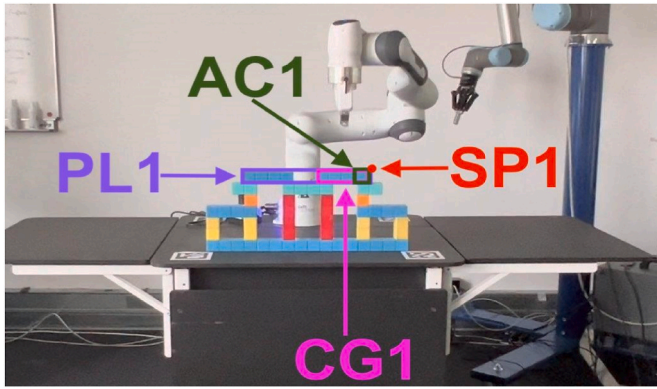


Fig. 8. Modeling concepts of ShellAssemblyRobotRAGs within the falsework. SP - support point, AC - atomic component, CG - component group, PL - product layer.

4.2.2. Shell structure assembly (Activity 2)

For an initial feasibility study of the shell structure assembly, a sequence of tasks was created by manually guiding the Franka Emika robot, defining the trajectory of the movement and the final position of the gripper. For this guidance, the Franka UI was used. Fully automating the shell assembly is possible, however, at the moment, the places of the shell modules resting on spatial support points of the falsework are not designed perfectly well. Therefore, hazards occur more easily. For a reduction of the hazards, shell modules should be designed taking the spatial support points into account so that they can be laid fittingly. However, this means that their design and production should be individually adapted to the support structure so that they immediately fit on the support points. This is considered to be a challenge for future work.

For each segment of the shell structure one task was taught, created with the Franka UI. A task consists of smaller sub-tasks like joint moves, linear moves, gripper openings, gripper closings, or moving to contact. The resulting process is depicted in Fig. 9, which shows photographs of the various stages of construction.

The arch assembly involves 14 components and requires a total assembly time of 808 s. Step durations for the arch range from 39 to 69 s, with an average of 57.7 s.

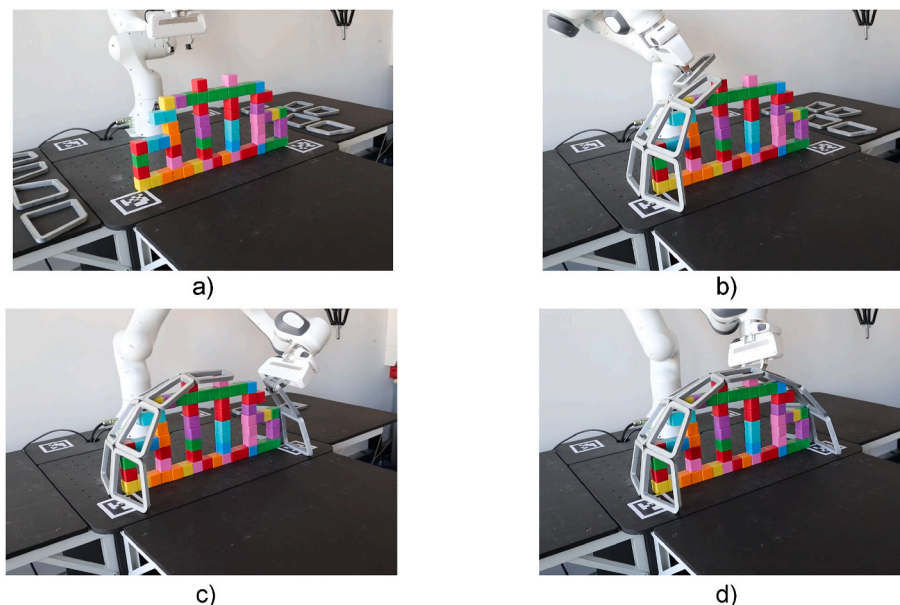


Fig. 9. Photographs of different stages of robotic assembly of a modular arch using falsework: a) assembled falsework, b) and c) installation of arch modules, and d) assembled arch.

4.2.3. Disassembly of the falsework (Activity 3)

Because RobotRAG stores all assembly actions in its history, the positions of all parts of a falsework, be they *AtomicComponents* or *ComponentGroups*, are known after the assembly. Since the assembly algorithm assembles all *ComponentGroups* layer-by-layer, it seems to be straightforward to synthesize a layer-wise disassembly by inverting the assembly algorithm of a RobotRAG. To this end, experiments are ongoing.

To reduce the number of potential hazards during disassembly and to avoid collisions between the robot arm and assembled shell modules in the arch-like shell, hydraulic scissor lifting platforms (Ciupan et al., 2019) can be used to enable automated lowering of the falsework after the completion of the shell assembly. In the case of the demonstrator, the support structure could be mounted on a movable lifting platform, and removed with its help from under the arch before dismantling.

4.3. Numerical analysis of the critical states during the assembling process

Modules from the shell structure presented in Fig. 5a with a thickness of 40 mm were evaluated for different stages of the assembling process. The material parameters were chosen based on the test results of Strain Hardening Cementitious Composite used to print the outer edges of the modules (Ivaniuk et al., 2022c), see Section 2.3. The material of the modules was defined using a linear-elastic constitutive law with Young's modulus of 23 GPa and Poissons' ratio of 0.2 assuming the uncracked state of the concrete. As the deformations were in the small strain regime, a linear strain-displacement relation was assumed. All computations were done in MATLAB 2023b.

In the assembling process, two main factors need to be considered, that can affect the impact of the assembling process on each module. First, the location where the gripper grabs the module can highly affect the module's vulnerability. Second, the orientation in space with the loading due to self-weight and the corresponding inertial forces due to acceleration by the robot.

To demonstrate the influence of the gripping position, the module depicted in Fig. 5b supported in three different positions was analyzed. It is important to note that only support positions where the module can be picked up by the gripper during assembly were considered. Three possible gripping positions are considered here as examples, see Fig. 10a). Fig. 10 b)-d) show the corresponding plots of the deformation

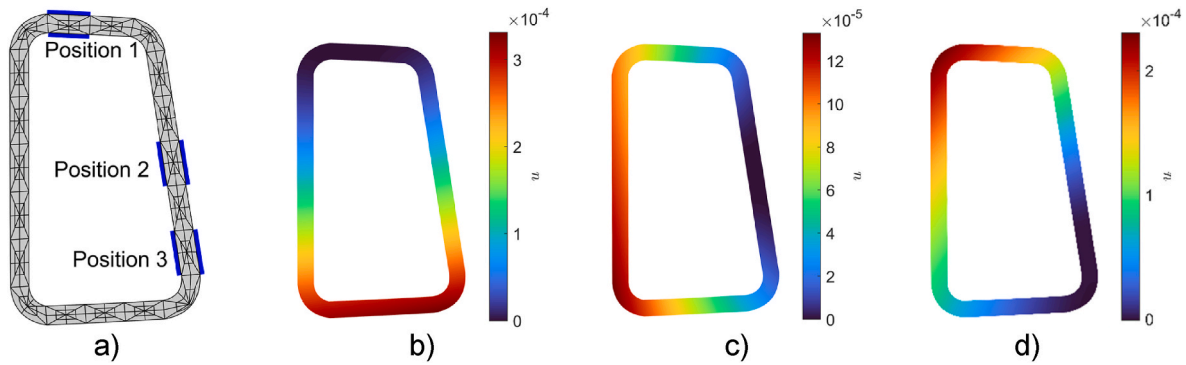


Fig. 10. a) Positions of the gripper to elevate and move the shell module to be considered for the evaluation with deformations (in m) under self-weight due to b) Position 1, c) Position 2, and d) Position 3.

of the module under its own weight.

The deformation plots in Fig. 10 show a large difference in the maximum deformation of the shell module, indicating that the gripper position should not be neglected. The maximum deflections in the module when held by the gripper in Position 1 are more than twice the deflections of the module when gripped in Position 2.

Besides the deformations, the stresses occurring in the module must also be taken into account. The bending stresses due to gripper Position 2 are depicted in Fig. 11.

The bending stresses are shown for the main bending stresses m_{11} and m_{22} such as the twisting moment m_{12} . The diagrams reveal that the stresses are especially high at the gripper position and superpose in the vicinity. Indeed, a precise investigation of the boundary conditions due to the grippers is pending and has an influence on the bending stresses e. g., a soft support might relax the stresses, however, it needs to be validated with experimental data to be applied.

During the robot-assisted assembly, each possible way of movement of the shell module should be investigated at the critical points of maximal acceleration and every time the orientation is changed. As an example, the right lower module of the shell shown in Fig. 5a has been analyzed, the geometry of which is presented in Fig. 12a. Fig. 12 b) shows the deformations of this module due to self-weight at the different stages of assembly. As can be seen, the deformations depend on the orientation of the module in space, which suggests that the trajectory of the module should also be taken into account.

For large-scale construction, it is especially necessary to analyze the stresses occurring in the modules while taking into account the acceleration during robot movement. To demonstrate this, an enlarged analog of the module shown in Fig. 5b we analyzed, whose dimensions are more realistic for use in the construction of large-scale shells. Fig. 13 shows the module geometry and the corresponding bending stresses m_{11}

due to 1) self-weight and 2) self-weight and the additional force caused by the acceleration of the robot at the point of the initial lifting in a horizontal position in the quasi-static simulation. It is assumed that the robot is able to move with acceleration in the range of 0–3 m/s², and the maximum value is used in the example.

The results of Fig. 13 show that the bending stresses m_{11} reach their maximum values in the areas close to the gripper. In terms of Cauchy stresses, neglecting the superposition of the bending stresses, the maximal value of the stress component σ_{11} due to the bending stresses m_{11} can be determined as 2.78 MPa without acceleration and 3.63 MPa considering acceleration. This shows that the emerging stresses can exceed the stresses at which cracks begin to form in the material (~3.5 MPa (Ivaniuk et al., 2022c)) when acceleration comes into play. Consequently, a reduction of the acceleration during the assembling can avoid module damage and maintain a crack-free state of the concrete, which is even more important when considering a superposition of the bending stresses. Hence, the interplay of structural analysis and robot-supported assembling is beneficial since recommendations can be given from the side of the structural analysis for the assembling in terms of limitations for the acceleration, the placement of the gripper, and the assembling path of the modules.

Prospectively, if the load-bearing capacity of the concrete modules exceeds the crack-free state or to consider reinforcement, constitutive relations for reinforced concrete can be incorporated in terms of a representative volume element (RVE) such as presented in (Mester et al., 2024) for Reissner-Mindlin shell theory. The application of an RVE in combination with Kirchhoff's theory is possible.

4.4. Discussion

In the tests conducted on the automated assembly of the

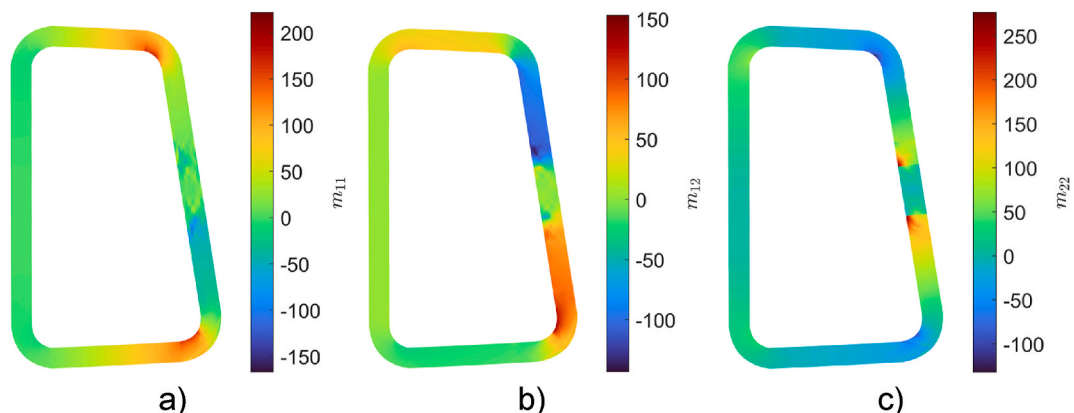


Fig. 11. Corresponding bending stresses (in Nm/m) due to self-weight and gripper Position 2 with a) m_{11} , b) m_{12} , and c) m_{22} .

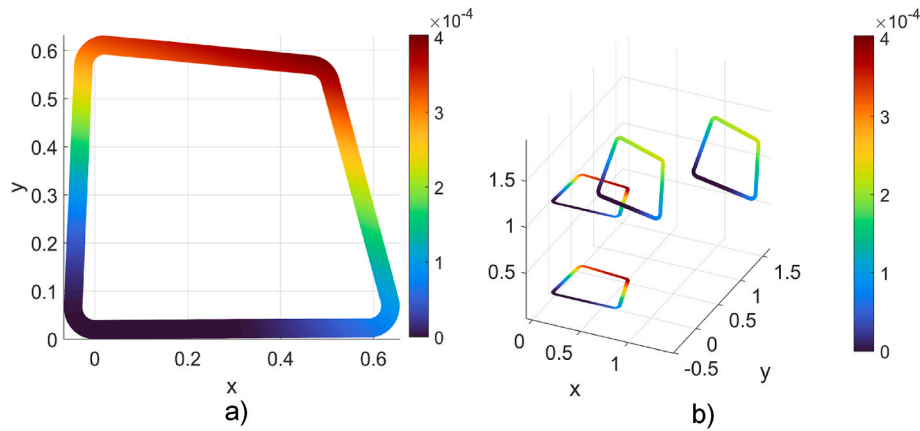


Fig. 12. Deformation magnitude (in m) of a shell module during the assembly using a gripper holding the module in the lower left corner: a) deformation in the initial lifting state and b) deformation magnitude at different stages of assembly.

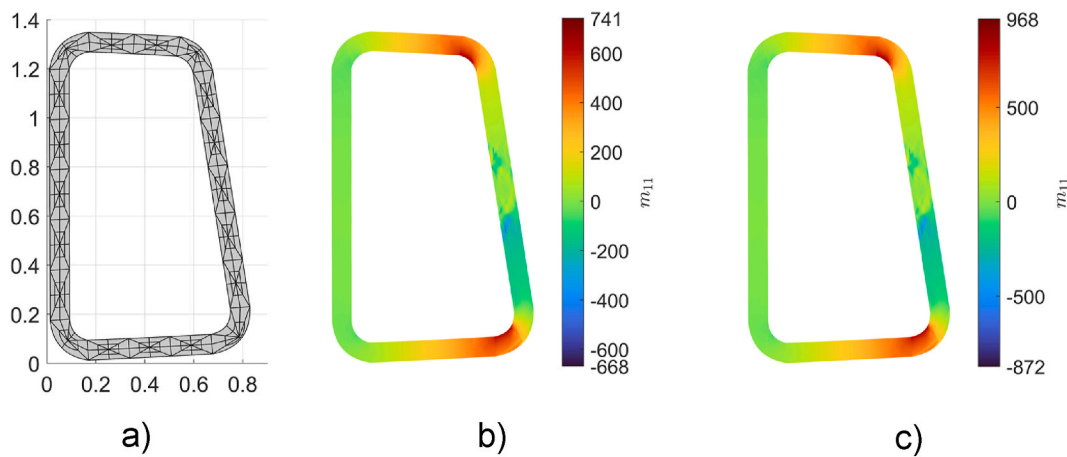


Fig. 13. a) Geometry of the module for large-scale construction (in m), and bending stresses m_{11} (in Nm/m) in the module gripped in Position 2 due to b) self-weight, and c) self-weight plus robot acceleration.

demonstrator, the time to install the falsework was 497 s, and the time to assemble the shell was 808 s. The disassembly of the falsework, performed in reverse order, takes approximately the same amount of time as its assembly. Based on this assumption, it can be concluded that, for the presented demonstrator, the use of the falsework extends the construction process by a factor of 2.2 compared to the time required solely for shell assembly, as is needed in the case of assembling the arch using a falsework-free automated assembly method involving two robots. However, it is important to note that magnets were employed to connect the modules of the arch, which is one of the fastest connection methods but is hardly suitable for large-scale applications. The use of other joining methods such as mechanical fasteners, welding, grouting, or adhesive bonding, would significantly increase the time of shell assembly, thus reducing the time difference between the two approaches. On the other hand, the assembly and disassembly of modular falsework can also require additional time, depending on the speed of module installation and the time needed to set up and adjust the height of the underlying lifting platform.

This work is a step towards a full-fledged digital twin in robotic assembly. In its current state, our approach models the real-time structure of physical components with the WorkCell model. Moreover, robotic skills and capabilities are covered by the RobotCapability model.

To achieve a full-fledged digital twin, additional enhancements are required. Firstly, more sensors such as cameras or LIDARs must be integrated to read a complete world model. Secondly, in contrast to the current stepwise approach, a bidirectional communication between the

simulation and physical environments must be developed. Finally, a compensation mechanism for solving cyber-physical inconsistency issues is of the utmost importance.

The presented approach can also be reused in areas beyond shell assembly or even robotic assembly. Modeling the robots' capabilities and skills allows them to be replaced for a different scenario without changing the general workflow. For example, pick and place skills modeled in ShellAssemblyRobotRAGs can be replaced by painting or polishing skills.

5. Summary and outlook

This publication presents a new alternative approach to the robotic construction of modular concrete shells using automatically assembled falsework. The presence of the falsework enables the construction of shells with large spans and complex geometries, and at the same time has the potential to improve the positioning accuracy of the modules. In the mid-term future, the use of modular falsework will support its assembly and disassembly by robots, enabling full automation of the construction process. The conducted experiments on the automated assembly of the manufactured demonstrator have shown the feasibility of the proposed approach.

The paper also analyzed the critical states in which the frame module may occur in the process of automated assembly using a gripper. The analysis showed that especially for large-scale assembling the health of the modules can be maintained by ensuring movement without reaching

the crack limit state of the modules. Therefore, several numerical examples underline crucial points during the construction process such as the gripper position, the module geometry, the construction path, and the acceleration.

This publication presents the first steps towards the realization of the proposed approach for automated assembly of modular shells using falsework, however, to enable the construction of large-scale shells, a number of developments are required. A modular falsework capable of supporting large modular shells needs to be developed. The connection between the falsework modules must be suitable for robotic assembly and disassembly. It is also necessary to develop a method of lowering the falsework after the shell has been assembled, which can be accomplished, for example, by using hydraulic scissor lifting platforms. Last but not least, a method of connecting shell modules suitable for robotic assembly needs to be developed.

CRedit authorship contribution statement

Egor Ivaniuk: Writing – review & editing, Writing – original draft, Visualization, Methodology, Investigation, Conceptualization. **Dmytro Pukhkaiev:** Writing – review & editing, Writing – original draft, Visualization, Supervision, Conceptualization. **Mathias Reichle:** Writing – original draft, Visualization, Software, Methodology, Investigation, Conceptualization. **Wanqi Zhao:** Writing – original draft, Visualization, Validation, Software, Methodology, Investigation. **Johannes Mey:** Writing – original draft, Software. **Manuel Krombolz:** Writing – original draft, Visualization, Validation, Software, Investigation. **Zlata Tosić:** Writing – original draft, Visualization, Methodology. **Uwe Aßmann:** Writing – review & editing, Writing – original draft, Supervision, Resources, Project administration, Funding acquisition, Conceptualization. **Sven Klinkel:** Supervision, Resources, Project administration, Funding acquisition, Conceptualization. **Viktor Mechtcherine:** Writing – review & editing, Supervision, Resources, Project administration, Funding acquisition, Conceptualization.

Declaration of competing interest

The authors declare that they have no known competing financial interests or personal relationships that could have appeared to influence the work reported in this paper.

Acknowledgment

The authors would like to thank the German Research Foundation (Deutsche Forschungsgemeinschaft – DFG) for financial support of project number 424057211 “Adaptive Concrete Diamond Construction (ACDC)”, within the Priority Program “Adaptive modularized constructions made in flux” (SPP 2187), the research unit FOR 5492: “Polytope Mesh Generation and Finite Element Analysis Methods for Problems in Solid Mechanics” under project number 495926269, and the Project ID 390696704, within the Cluster of Excellence “Centre for Tactile Internet with Human-in-the-Loop” (CeTI) of Technische Universität Dresden (EXC 2050/1).

The authors acknowledge the financial support by the Federal Ministry of Education and Research of Germany in the program “Souverän. Digital. Vernetzt.”. Joint project 6G-life, project identification number: 16KISK001K.

In addition, the authors acknowledge the financial support of the research project DigiPhenoMS funded by the Free State of Saxony, Germany (Funding Guideline: eHealthSax).

This research was also supported by funding from ESF Plus and the Free State of Saxony (Nr. 100687967).

Data availability

No data was used for the research described in the article.

References

- Abdelmagid, A., Tosić, Z., Mirani, A., et al., 2023. Design Model for Block-Based Structures from Triply Orthogonal Systems of Surfaces, pp. 165–176.
- Aghazadeh, S., Hafeznezami, S., Najjar, L., Huq, Z., 2011. The influence of work-cells and facility layout on the manufacturing efficiency. *J. Facil. Manag.* 9, 213–224. <https://doi.org/10.1108/14725961111148117>.
- Ahmad, M., 2017. An Ontology-Based Approach for Integrating Engineering Workflows for Industrial Assembly Automation Systems. University of Warwick. Doctoral Thesis.
- Ahmad, M., Ferrer, B.R., Ahmad, B., et al., 2018. Knowledge-based PPR modelling for assembly automation. *CIRP Journal of Manufacturing Science and Technology* 21, 33–46. <https://doi.org/10.1016/j.cirpj.2018.01.001>.
- Arf, J., Reichle, M., Klinkel, S., Simeon, B., 2023. Scaled boundary isogeometric analysis with C1 coupling for Kirchhoff plate theory. *Comput. Methods Appl. Mech. Eng.* 415. <https://doi.org/10.1016/j.cma.2023.116198>.
- Arioli, C., Shamanskiy, A., Klinkel, S., Simeon, B., 2019. Scaled boundary parametrizations in isogeometric analysis. *Comput. Methods Appl. Mech. Eng.* 349, 576–594. <https://doi.org/10.1016/j.cma.2019.02.022>.
- Bauer, B., Arioli, C., Simeon, B., 2021. Generating star-shaped blocks for scaled boundary multipatch IGA. In: van Brummelen, H., Vuik, C., Möller, M., et al. (Eds.), *Isogeometric Analysis and Applications 2018*. Springer International Publishing, Cham, pp. 1–25.
- Beaulieu, A., Givigi, S.N., Ouellet, D., Turner, J.T., 2018. Model-driven development architectures to solve complex autonomous robotics problems. *IEEE Syst. J.* 12, 1404–1413. <https://doi.org/10.1109/JSYST.2016.2583403>.
- Bhooshan, S., Bhooshan, V., Dell’Endice, A., et al., 2022. The Striatum bridge: computational design and robotic fabrication of an unreinforced, 3D-concrete-printed, masonry arch bridge. *Archit Struct Constr* 2, 521–543. <https://doi.org/10.1007/s44150-022-00051-y>.
- Block, P., Ochsendorf, J., 2007. Thrust network analysis: a new methodology for three-dimensional equilibrium. *Journal of the International Association for Shell and Spatial Structures* 48.
- Bock, T., 2015. The future of construction automation: technological disruption and the upcoming ubiquity of robotics. *Autom. Construct.* 59, 113–121. <https://doi.org/10.1016/j.autcon.2015.07.022>.
- Bruun, E.P.G., Pastrana, R., Paris, V., et al., 2021. Three cooperative robotic fabrication methods for the scaffold-free construction of a masonry arch. *Autom. Construct.* 129. <https://doi.org/10.1016/j.autcon.2021.103803>.
- BT-Spannschloss® - Connecting precast concrete parts securely. In: *Technologien und Beratung für den Betonbau - B.T. innovation*. <https://www.bt-innovation.de/en/products/connecting-systems/bt-spannschloss/>. Accessed 2 September 2024.
- Chasapi, M., Klinkel, S., 2018. A scaled boundary isogeometric formulation for the elasto-plastic analysis of solids in boundary representation. *Comput. Methods Appl. Mech. Eng.* 333, 475–496. <https://doi.org/10.1016/j.cma.2018.01.015>.
- Chen, Z., Bao, J., Zheng, X., Liu, T., 2020. Assembly information model based on knowledge graph. *J. Shanghai Jiao Tong Univ. (Sci.)* 25, 578–588. <https://doi.org/10.1007/s12204-020-2179-y>.
- Ciupan, C., Ciupan, E., Pop, E., 2019. Algorithm for designing a hydraulic scissor lifting platform. *MATEC Web Conf* 299. <https://doi.org/10.1051/mateconf/201929903012>.
- Coleman, D., Sucan, I., Chitta, S., Correll, N., 2014. Reducing the Barrier to Entry of Complex Robotic Software: a MoveIt! Case Study.
- Costa, E., Oval, R., Shepherd, P., Orr, J., 2021. Fabrication-aware parametric design of segmented concrete shells. In: *Proceedings of the IASS Annual Symposium 2020/21 and the 7th International Conference on Spatial Structures: Inspiring the Next Generation*.
- Cutting-Decelle, A.F., Young, R.I.M., Michel, J.J., et al., 2007. ISO 15531 mandate: a product-process-resource based approach for managing modularity in production management. *Concurr. Eng.* 15, 217–235. <https://doi.org/10.1177/1063293X07079329>.
- Dantam, N., Kolhe, P., Stilman, M., 2011. The Motion Grammar for physical human-robot games. In: 2011 IEEE International Conference on Robotics and Automation, pp. 5463–5469.
- Davis, L., Rippmann, M., Pawlofsky, T., Block, P., 2012. Innovative funicular tile vaulting: a prototype in Switzerland. *Struct. Eng.* 90, 46–56.
- De Fazio, T., Whitney, D., 1987. Simplified generation of all mechanical assembly sequences. *IEEE J. Robot. Autom.* 3, 640–658. <https://doi.org/10.1109/JRA.1987.1087132>.
- Dehnavi, S., Sedaghatbaf, A., Salmani, B., et al., 2019. Towards an actor-based approach to design verified ROS-based robotic programs using rebecca. *Procedia Comput. Sci.* 155, 59–68. <https://doi.org/10.1016/j.procs.2019.08.012>.
- Deuss, M., Panozzo, D., Whiting, E., et al., 2014. Assembling self-supporting structures. *ACM Trans. Graph.* 33, 1–10. <https://doi.org/10.1145/2661229.2661266>.
- Dimic, M., 2011. Structural Optimization of Grid Shells Based on Genetic Algorithms. Universität Stuttgart. Doctoral Thesis.
- Dini, G., Santochi, M., 1992. Automated sequencing and subassembly detection in assembly planning. *CIRP Annals* 41, 1–4. [https://doi.org/10.1016/S0007-8506\(07\)61140-8](https://doi.org/10.1016/S0007-8506(07)61140-8).
- Dombernowsky, P., Sondergaard, A., 2009. Three-dimensional topology optimisation in architectural and structural design of concrete structures. In: *Proceedings of the International Association for Shell and Spatial Structures (IASS) Symposium 2009*, pp. 1066–1077. Valencia.
- Douthe, C., Mesnil, R., Orts, H., Baverel, O., 2017. Isoradial meshes: covering elastic gridshells with planar facets. *Autom. Construct.* 83, 222–236. <https://doi.org/10.1016/j.autcon.2017.08.015>.

- Ebert, S., Mey, J., Schöne, R., et al., 2023. DiNeROS: A Model-Driven Framework for Verifiable ROS Applications with Petri Nets. *IEEE, Västerås, Sweden*.
- Ebert, S., Mey, J., Schöne, R., et al., 2024. Distributed Petri nets ROS. *Innovat. Syst. Software Eng.* <https://doi.org/10.1007/s11334-024-00570-5>.
- ElMaraghy, H., ElMaraghy, W., 2016. Smart adaptable assembly systems. *Procedia CIRP* 44, 4–13. <https://doi.org/10.1016/j.procir.2016.04.107>.
- Gabriel, F., Fahning, M., Meiners, J., et al., 2020. Modeling of vacuum grippers for the design of energy efficient vacuum-based handling processes. *Prod. Eng. Res. Dev.* 14, 545–554. <https://doi.org/10.1007/s11740-020-00990-9>.
- Gazebo. <https://gazebo.org/about>. (Accessed 15 December 2024).
- Gericke, O., Kovaleva, D., Haase, W., Sobek, W., 2016. Fabrication of concrete parts using a frozen sand formwork. *Proceedings of the IASS Annual Symposium 2016 “Spatial Structures in the 21st Century* 141, 1–10.
- Görner, M., Haschke, R., Ritter, H., Zhang, J., 2019. MoveIt! Task constructor for task-level motion planning. In: *2019 International Conference on Robotics and Automation (ICRA)*, pp. 190–196.
- Groenewolt, A., Schwinn, T., Nguyen, L., Menges, A., 2018. An interactive agent-based framework for materialization-informed architectural design. *Swarm Intell* 12, 155–186. <https://doi.org/10.1007/s11721-017-0151-8>.
- Gu, P., Yan, X., 1995. CAD-directed automatic assembly sequence planning. *Int. J. Prod. Res.* 33, 3069–3100. <https://doi.org/10.1080/00207549508904862>.
- Hadj, R.B., Belhadj, I., Trigui, M., Aifaoui, N., 2018. Assembly sequences plan generation using features simplification. *Adv. Eng. Software* 119, 1–11. <https://doi.org/10.1016/j.advengsoft.2018.01.008>.
- Hammad, A., Akbarnezhad, A., 2017. *Modular vs Conventional Construction: A Multi-Criteria Framework Approach*. Taipei, Taiwan.
- Hawkins, W.J., Herrmann, M., Ibell, T.J., et al., 2016. Flexible formwork technologies – a state of the art review. *Struct. Concr.* 17, 911–935. <https://doi.org/10.1002/suco.201600117>.
- Holland, W van, Bronsvort, W.F., 2000. Assembly features in modeling and planning. *Robot. Comput. Integrated Manuf.* 16, 277–294. [https://doi.org/10.1016/S0736-5845\(00\)00014-4](https://doi.org/10.1016/S0736-5845(00)00014-4).
- Homem de Mello, L.S., Sanderson, A.C., 1988. Automatic generation of mechanical assembly sequences. *Carnegie Mellon University, Ne Robotics Institute. Carnegie Mellon University*.
- Homem de Mello, L.S., Sanderson, A.C., 2002. AND/OR graph representation of assembly plans. *IEEE Trans. Robot. Autom.* 6, 188–199. <https://doi.org/10.1109/70.54734>.
- Hořínková, D., 2021. Advantages and disadvantages of modular construction, including environmental impacts. *IOP Conf. Ser. Mater. Sci. Eng.* 1203, 032002. <https://doi.org/10.1088/1757-899X/1203/3/032002>.
- Ivaniuk, E., Tošić, Z., Eichenauer, M.F., et al., 2022a. Automated production of textile reinforced concrete modules for the assembly of shell structures. In: *14th Fib Phd Symposium in Civil Engineering, Rome, Italy*, pp. 763–770.
- Ivaniuk, E., Eichenauer, F.M., Tošić, Z., et al., 2022b. 3D printing and assembling of frame modules using printable strain-hardening cement-based composites (SHCC). *Mater. Des.* 219. <https://doi.org/10.1016/j.matdes.2022.110757>.
- Ivaniuk, E., Ivanova, I., Sokolov, D., et al., 2022c. Application-driven material design of printable strain hardening cementitious composites (SHCC). *Materials* 15. <https://doi.org/10.3390/ma15051631>.
- Ivaniuk, E., Tošić, Z., Müller, S., et al., 2024. Automated manufacturing of reinforced modules of segmented shells based on 3D printing with strain-hardening cementitious composites. *Autom. ConStruct.* 166. <https://doi.org/10.1016/j.autcon.2024.105591>.
- Kao, G., Körner, A., Sonntag, D., et al., 2017. Assembly-aware design of masonry shell structures: a computational approach. In: *Proceedings of the IASS Annual Symposium 2017 “Interfaces: Architecture, engineering, science*.
- Kao, G.T.-C., Iannuzzo, A., Thomaszewski, B., et al., 2022. Coupled rigid-block analysis: stability-aware design of complex discrete-element assemblies. *Comput. Aided Des.* 146. <https://doi.org/10.1016/j.cad.2022.103216>.
- Knepper, R.A., Layton, T., Romanishin, J., Rus, D., 2013. IkeaBot: an autonomous multi-robot coordinated furniture assembly system. In: *2013 IEEE International Conference on Robotics and Automation*, pp. 855–862.
- Kromoser, B., Huber, P., 2016. Pneumatic formwork systems in structural engineering. *Adv. Mater. Sci. Eng.* 2016. <https://doi.org/10.1155/2016/4724036>.
- Kumar, P., Patnaik, A., Chaudhary, S., 2017. A review on application of structural adhesives in concrete and steel-concrete composite and factors influencing the performance of composite connections. *Int. J. Adhesion Adhes.* 77, 1–14. <https://doi.org/10.1016/j.ijadhadh.2017.03.009>.
- Lauer, A.P.R., Benner, E., Stark, T., et al., 2023. Automated on-site assembly of timber buildings on the example of a biomimetic shell. *Autom. ConStruct.* 156. <https://doi.org/10.1016/j.autcon.2023.105118>.
- Lazzerini, B., Marcelloni, F., 2000. A genetic algorithm for generating optimal assembly plans. *Artif. Intell. Eng.* 14, 319–329. [https://doi.org/10.1016/S0954-810\(00\)00011-X](https://doi.org/10.1016/S0954-810(00)00011-X).
- Liew, J.Y.R., Chua, Y., Dai, Z., 2019. Steel concrete composite systems for modular construction of high-rise buildings. *Structures* 21. <https://doi.org/10.1016/j.istruc.2019.02.010>.
- Liu, R., Sun, Y., Liu, C., 2023. Robotic LEGO Assembly and Disassembly from Human Demonstration.
- Luitse, S., Eigenraam, P., 2017. Reverse deconstruction: a method for optimized assembly of prefab shell structures. In: *Proceedings of IASS Annual Symposia 2017*, pp. 1–9.
- Lupinetti, K., Pernot, J.-P., Monti, M., Giannini, F., 2019. Content-based CAD assembly model retrieval: survey and future challenges. *Comput. Aided Des.* 113, 62–81. <https://doi.org/10.1016/j.cad.2019.03.005>.
- Macenski, S., Foote, T., Gerkey, B., et al., 2022. Robot operating system 2: design, architecture, and uses in the wild. *Sci. Robot.* 7. <https://doi.org/10.1126/scirobotics.abm6074>.
- Mainka, J., Kloft, H., Stein, E., Wirth, F., 2017. Non-Waste wax formwork-technology: innovative precision formwork for concrete members made of recyclable industrial waxes. In: *Proceedings of IASS Annual Symposia 2017*, pp. 1–10.
- Man, H., Song, C., Xiang, T., et al., 2013. High-order plate bending analysis based on the scaled boundary finite element method. *Int. J. Numer. Methods Eng.* 95, 331–360. <https://doi.org/10.1002/nme.4519>.
- Manzini, M., Unglert, J., Gyulai, D., et al., 2018. An integrated framework for design, management and operation of reconfigurable assembly systems. *Omega* 78, 69–84. <https://doi.org/10.1016/j.omega.2017.08.008>.
- Mester, L., Klarmann, S., Klinkel, S., 2024. Homogenization assumptions for the two-scale analysis of first-order shear deformable shells. *Comput. Mech.* 73, 795–829. <https://doi.org/10.1007/s00466-023-02390-z>.
- Mey, J., Schöne, R., Hedin, G., et al., 2020. Relational reference attribute grammars: improving continuous model validation. *Journal of Computer Languages* 57. <https://doi.org/10.1016/j.cola.2019.100940>.
- Nägele, L., Schierl, N., Hoffmann, A., Reif, W., 2024. Modular and Domain-Guided Multi-Robot Planning for Assembly Processes, pp. 595–604.
- Nordmann, A., Hochgeschwender, N., Wrede, S., 2014. A survey on domain-specific languages in robotics. In: *Brugali, D., Broenink, J.F., Kroeger, T., MacDonald, B.A. (Eds.), Simulation, Modeling, and Programming for Autonomous Robots. Springer International Publishing, Cham*, pp. 195–206.
- Oval, R., Nuh, M., Costa, E., et al., 2023. A prototype low-carbon segmented concrete shell building floor system. *Structures* 49, 124–138. <https://doi.org/10.1016/j.istruc.2023.01.063>.
- Paris, V., Lepore, N., Bruun, E., et al., 2021. Robotic construction of a self-balancing glass masonry vault: DEM study of stability during construction stages. In: *Proceedings of the IASS Annual Symposium 2020/21 and the 7th International Conference on Spatial Structures*. Guilford, UK.
- Park, H., Park, J., Lee, D.-H., et al., 2017. Compliance-based robotic peg-in-hole assembly strategy without force feedback. *IEEE Trans. Ind. Electron.* 64, 6299–6309. <https://doi.org/10.1109/TIE.2017.2682002>.
- Pellis, D., Kilian, M., Pottmann, H., Pauly, M., 2021. Computational design of weingarten surfaces. *ACM Trans. Graph.* 40, 114:1–114:11. <https://doi.org/10.1145/3450626.3459939>.
- Peters, S., Trummer, A., Amsberg, F., et al., 2017. Precast concrete shells: a structural challenge. *Fabricate* 250–257. <https://doi.org/10.2307/j.ctt1n7qkg7.38>.
- Pluta, K., Edelstein, M., Vaxman, A., Ben-Chen, M., 2021. PH-CPF: planar hexagonal meshing using coordinate power fields. In: *ACM Transactions on Graphics, ACM*, p. 156.
- Reichle, M., Arf, J., Simeon, B., Klinkel, S., 2023. Smooth multi-patch scaled boundary isogeometric analysis for Kirchhoff–Love shells. *Meccanica* 58, 1693–1716. <https://doi.org/10.1007/s11012-023-01692-z>.
- Reichle, M., Klassen, M., Li, J., Klinkel, S., 2024. A modified approach for a scaled boundary shell formulation in structural isogeometric analysis. *Eng. Anal. Bound. Elem.* 159, 81–94. <https://doi.org/10.1016/j.enganabound.2023.11.017>.
- Rippmann, M., Lachauer, L., Block, P., 2012. Interactive vault design. *Int. J. Space Struct.* 27, 219–230. <https://doi.org/10.1260/0266-3511.27.4.219>.
- Rippmann, M., Liew, A., Van Mele, T., Block, P., 2018. Design, fabrication and testing of discrete 3D sand-printed floor prototypes. *Mater. Today Commun.* 15, 254–259. <https://doi.org/10.1016/j.mtcomm.2018.03.005>.
- Rovida, F., Crosby, M., Holz, D., et al., 2017. SKiROS—a skill-based robot control platform on top of ROS. In: *Koubaa, A. (Ed.), Robot Operating System (ROS): the Complete Reference, vol. 2. Springer International Publishing, Cham*, pp. 121–160.
- Schipper, H.R., 2015. *Double-curved Precast Concrete Elements: Research into Technical Viability of the Flexible Mould Method*. Delft University of Technology. Doctoral Thesis.
- Schipper, H.R., Grunewald, S., Eigenraam, P., et al., 2014. Production of Curved Precast Concrete Elements for Shell Structures and Free-form Architecture Using the Flexible Mould Method, pp. 1–12.
- Schlegel, C., Hassler, T., Lotz, A., Steck, A., 2009. Robotic software systems: from code-driven to model-driven designs. In: *2009 International Conference on Advanced Robotics*, pp. 1–8.
- Scrivener, K., John, V., Gartner, E., 2018. Eco-efficient cements: potential economically viable solutions for a low-CO₂ cement-based materials industry. *Cement Concr. Res.* 114. <https://doi.org/10.1016/j.cemconres.2018.03.015>.
- Shah, A., Sahin, S., Malafey, A., et al., 2022. Assembly-oriented design methodology for segmented timber shells. *Innovation, sustainability, legacy*. In: *Proceedings of the IASS 2022 Symposium Affiliated with APCS 2022 Conference*.
- Shamshiri, A., Hefzi, S., Morchi, H., 2019. *Time Comparison between Precast and Conventional Construction: A Case Study of Iran Mall Parking*.
- Shilova, E., Murugesu, M., Weinstock, M., 2018. Robotic fabrication of segmented shells: integrated data-driven design. *Simulation* 50, 150–157. <https://doi.org/10.22360/simaud.2018.simaud.020>.
- Sitnikov, V., 2019. Ice formwork for high-performance concrete: a model of lean production for prefabricated concrete industry. *Structures* 18, 109–116. <https://doi.org/10.1016/j.istruc.2018.11.004>.
- Stavric, M., Kaftan, M., 2012. Robotic fabrication of modular formwork for non-standard concrete structures. *Digital physicality: Proceedings of the 30th eCAADe conference* 2, 421–428. Prague.
- Straten G van der, 2018. *Connecting Prefabricated Concrete Shell Segments*. Master Thesis.
- Sun, Z., Mei, H., Pan, W., et al., 2022. A robotic arm based design method for modular building in cold region. *Sustainability* 14. <https://doi.org/10.3390/su14031452>.

- Sung RCW, Corney JR, Clark DER (2001) Octree based assembly sequence generation. In: Proceedings of the Sixth ACM Symposium on Solid Modeling and Applications. Association for Computing Machinery, New York, NY, USA, pp 120–129.
- ten Pas, A., Gualtieri, M., Saenko, K., Platt, R., 2017. Grasp pose detection in point clouds. *Int. J. Robot Res.* 36, 1455–1473. <https://doi.org/10.1177/0278364917735594>.
- Tošić, Z., Eichenauer, M.F., Ivaniuk, E., et al., 2022. Design and optimization of free-form surfaces for modular concrete 3D printing. *Autom. ConStruct.* 141. <https://doi.org/10.1016/j.autcon.2022.104432>.
- Vatandoost, M., Ekhlasi, A., Golabchi, M., et al., 2024. Fabrication methods of shell structures. *Autom. ConStruct.* 165. <https://doi.org/10.1016/j.autcon.2024.105570>.
- Wagner, H.J., Alvarez, M., Groenewolt, A., Menges, A., 2020. Towards digital automation flexibility in large-scale timber construction: integrative robotic prefabrication and co-design of the BUGA Wood Pavilion. *Constr Robot* 4, 187–204. <https://doi.org/10.1007/s41693-020-00038-5>.
- Wang, J., Liu, W., Kao, G.T.-C., et al., 2023. Multi-robotic assembly of discrete shell structures. In: *Multi-Robotic Assembly of Discrete Shell Structures*. De Gruyter, pp. 261–274.
- Zhang, N., Qi, T., Zhao, Y., 2021. Real-time learning and recognition of assembly activities based on virtual reality demonstration. *Sensors* 21. <https://doi.org/10.3390/s21186201>.
- Zhao, W., Mey, J., Schöne, R., et al., 2023. RobotRAGs: a reference attribute grammar-based integration approach for robotic assembly lines. In: *2023 49th Euromicro Conference on Software Engineering and Advanced Applications (SEAA)*, pp. 22–29.